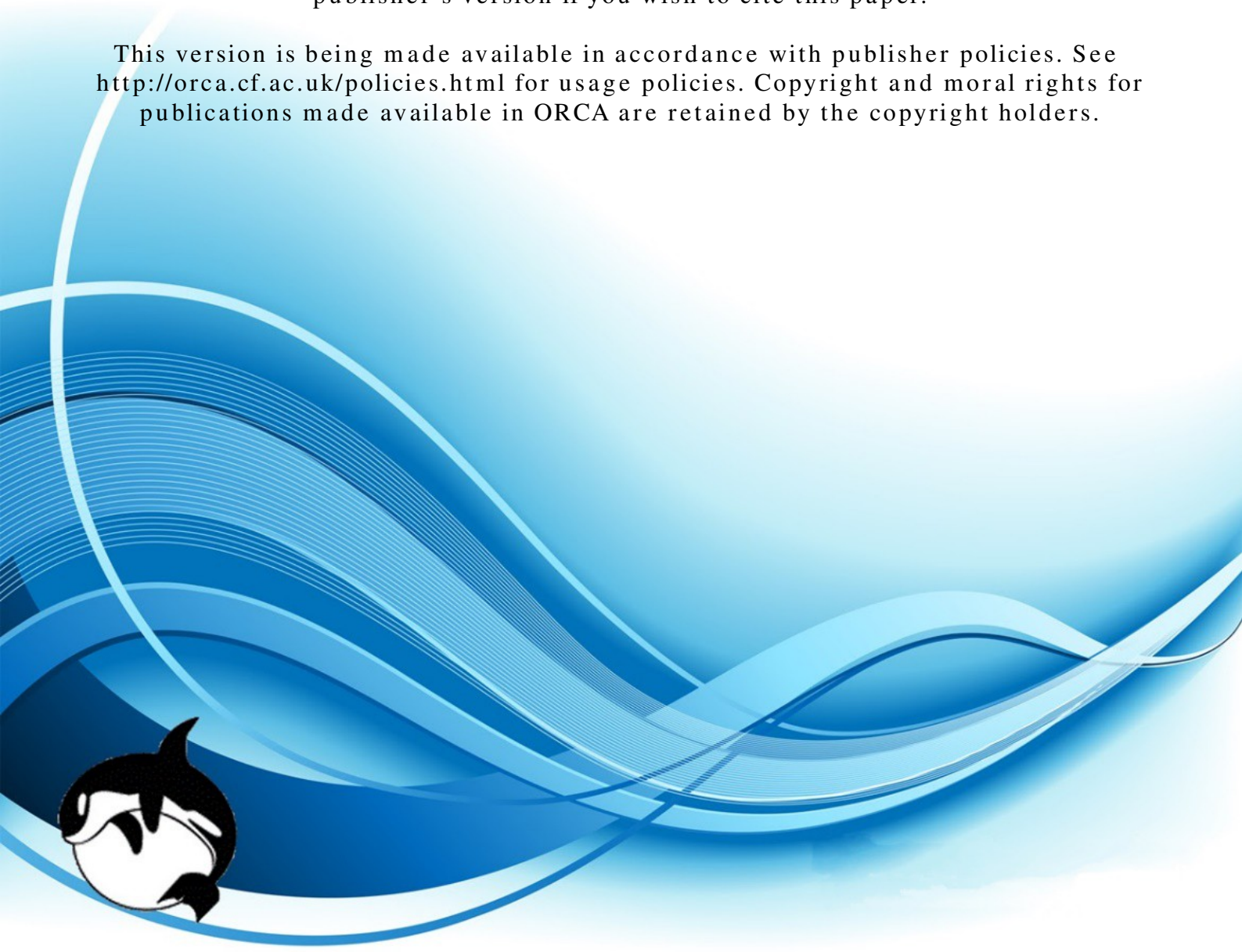

The X-ray Photoelectron Spectra of Ir, IrO_2 and $IrCl_3$ Revisited

Supplementary Information

S. J. Freakley, J. Ruiz-Esquius and D. J. Morgan*

Cardiff Catalysis Institute, School of Chemistry, Park Place, Cardiff. CF10 3AT. UK

*Corresponding author; Email: MorganDJ3@cardiff.ac.uk

Notes on Lineshapes

The choice of lineshape is of the utmost importance when constructing a peak model. Typically, the selection of lineshapes used in XPS is based on the combinations of Gaussian and Lorentzian (GL) functions that are used to model such photoelectron peaks, however the application of these peak shapes is typically for simplicity opposed to applicability, and lineshapes rarely conform to such mathematical forms.

For these reasons the LF lineshape considered is a more flexible functional form based on a Lorentzian shape modified and numerically convoluted with a Gaussian. Deriving from ideas introduced by Doniach-Sunjic asymmetric lineshapes, the LF lineshape is altered to force functional forms with finite area since infinite lineshapes are of limited practical use as intensity measurements are arbitrary and ill defined.

A Lorentzian lineshape with FWHM *f* and position (in kinetic energy) *e* is given by

$$L(x: f, e) = \frac{1}{1 + 4\left(\frac{x - e}{f}\right)^2}$$

The basis for both the LA and LF lineshapes in CasaXPS is

$$LA(x: \alpha, \beta, f, e) = \begin{cases} [L(x: f, e)]^{\alpha} & x \leq e \\ [L(x: f, e)]^{\beta} & x > e \end{cases}$$

The lineshape parameter entered on the Components property page of CasaXPS for the asymmetric Lorentzian is LA(α, β, *m*), where *m* is an integer between 0 and 499 defining the width of the Gaussian used to convolute the *LA* functional form.

Depending on the values chosen for the parameters α and β, the LA lineshape can define functional forms with infinite area. For this reason the LA definition is modified by an additional parameter to ensure the LF lineshape corresponds to a finite area.

LF(α, β, *w*, *m*) is identical to the LA lineshape with the exception that the specified values of α and β are force to increase to a constant value via a smooth function determined by the width parameter *w*. The examples in the workshop videos use the LF lineshape as the preferred lineshape where asymmetry is necessary for obtaining a good fit to a data envelope.

Further information on these and other asymmetric lienshapes can be found in reference [1] given at the foot of this document.

Figure S1: Characterisation of Iridium Oxides

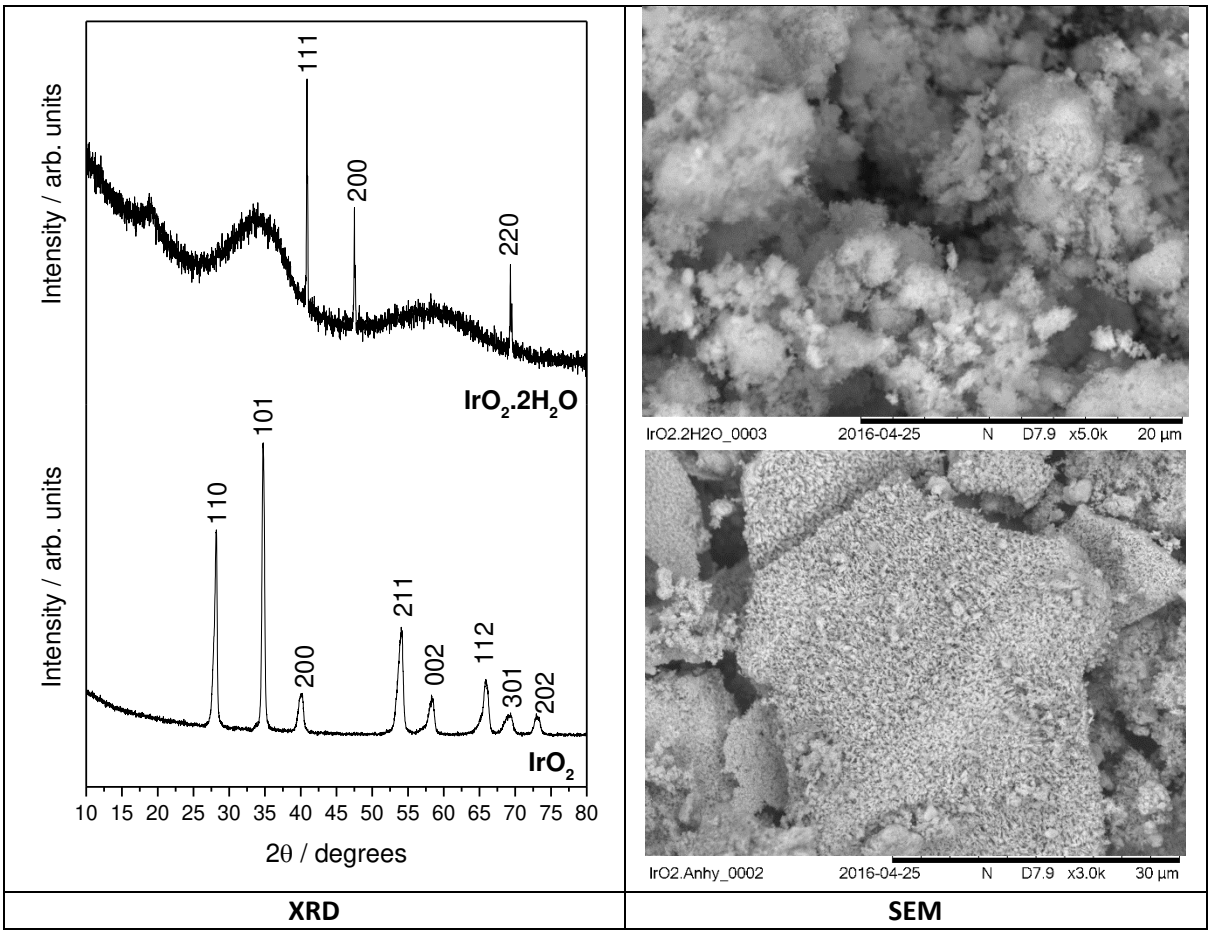

XRD | **SEM**

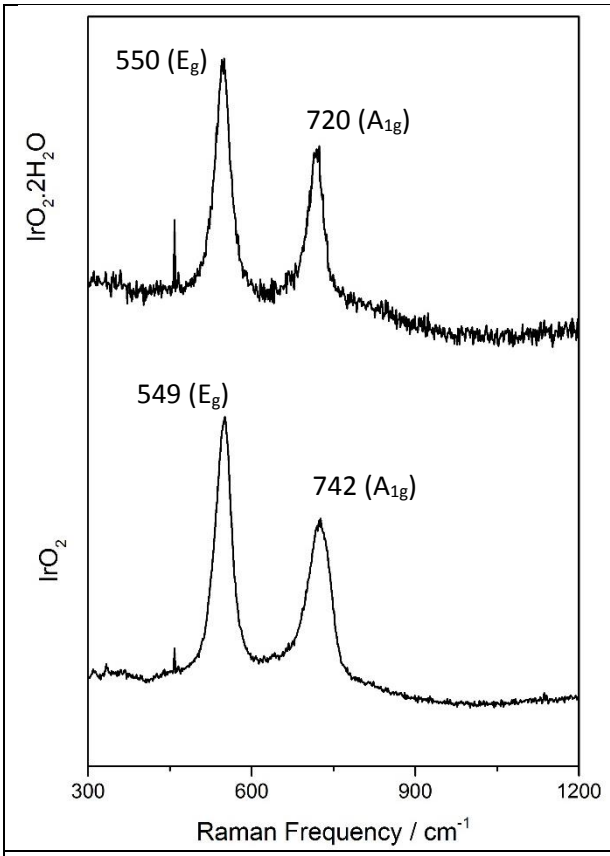
550 (E_g)
720 (A_{1g})
$IrO_2.2H_2O$
549 (E_g)
742 (A_{1g})
IrO_2
300
600
900
1200
Raman Frequency / cm^{-1}

Raman

SEM Characterisation of Iridium Chlorides

$IrCl_3.nH_2O$

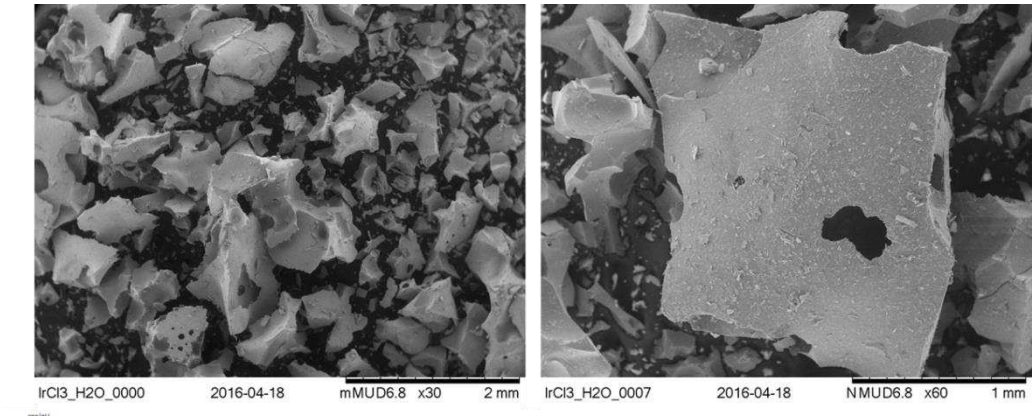

$IrCl_3$ (Anhydrous)

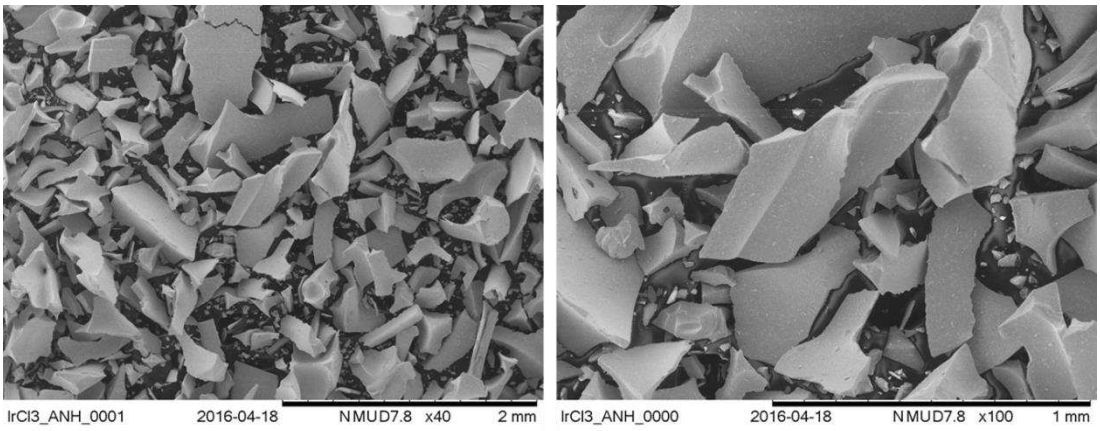

XRD, SEM and Raman analysis of the iridium oxides and chlorides used in the present study. XRD and SEM analysis of the oxides, are similar to those found by Pfeifer *et al.*[2]; specifically an amoprhous hydrated oxide with some metallic Ir reflections, whilst the anhydrous material exhibts reflections consistent with the rutile structure of IrO_2. Raman analysis of the oxides reveal bands consistent with IrO_2 of varying crystallinity. All values are shifted *ca.* 10 cm^{-1} downward from those measure for single crystal IrO_2.[3] SEM analysis of the chlorides revealed relatively flat shards of chloride, whilst the hydrated chloride exhibited much larger structures, with many exhibiting a "Swiss cheese" appearance from the many voids present.

Due to the hygroscopic nature of the chlorides, XRD and Raman analysis of the samples exhibited a large degree of oxidation and therefore their analysis has not been taken further.

Figure S2: Comparison of Fitting of the Ir(4f) region for metallic Ir with line shape derived from HAXPES studies. For clarity the Ir(5p) peak is excluded as per the HAXPES study.[2]

<table>
<tr>
<td> 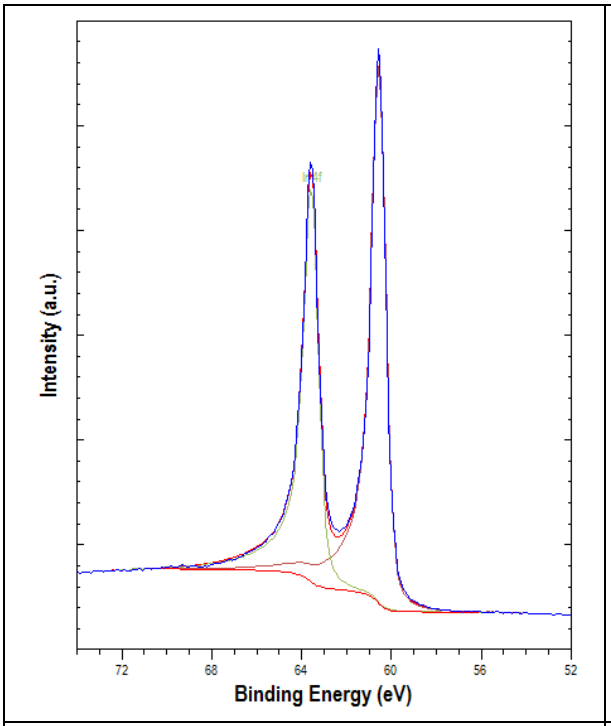
</td>
<td> 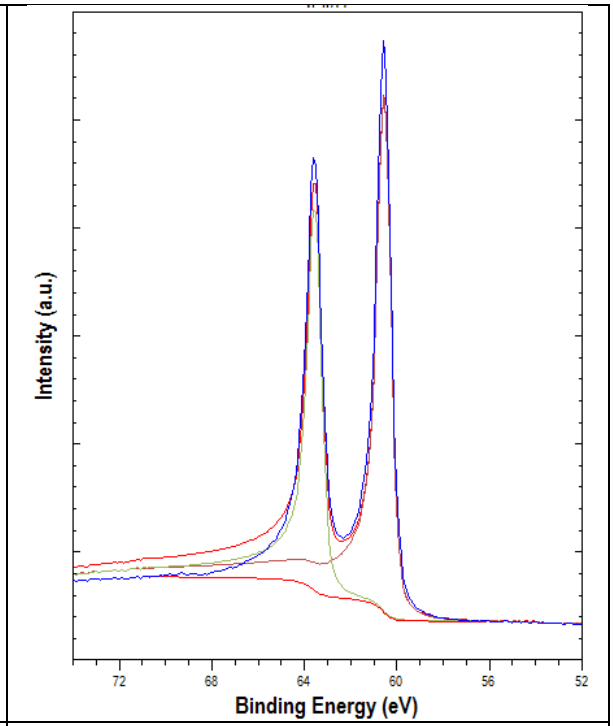
</td>
</tr>
<tr>
<td>Current fit, with the line shape derived in the main paper (LF(0.6,1,150,300))</td>
<td>Fitting as taken from reference [2]. The line shape (DS(0.13,250)SGL(90)), was selected as the closest for photon energy to a conventional lab source.</td>
</tr>
</table>

To check the validity of the fit, we have taken the ratio of the fitted components to that of the Ir(4d) level. The ratios are given below, with a value close to unity indicating excellent agreement.

	Ir(4f) Area%	Ir(4d) Area%	Ratio (4d/4f)
Total Corrected Area	51.95	48.05	1.09
DS(0.13,250) SGL(90) (From Ref [1])	41.83	58.17	0.72
LF(0.6,1,150,300) (Current Paper)	50.12	49.88	1.01

Figure S3: Fitting of Ir(4d) regions

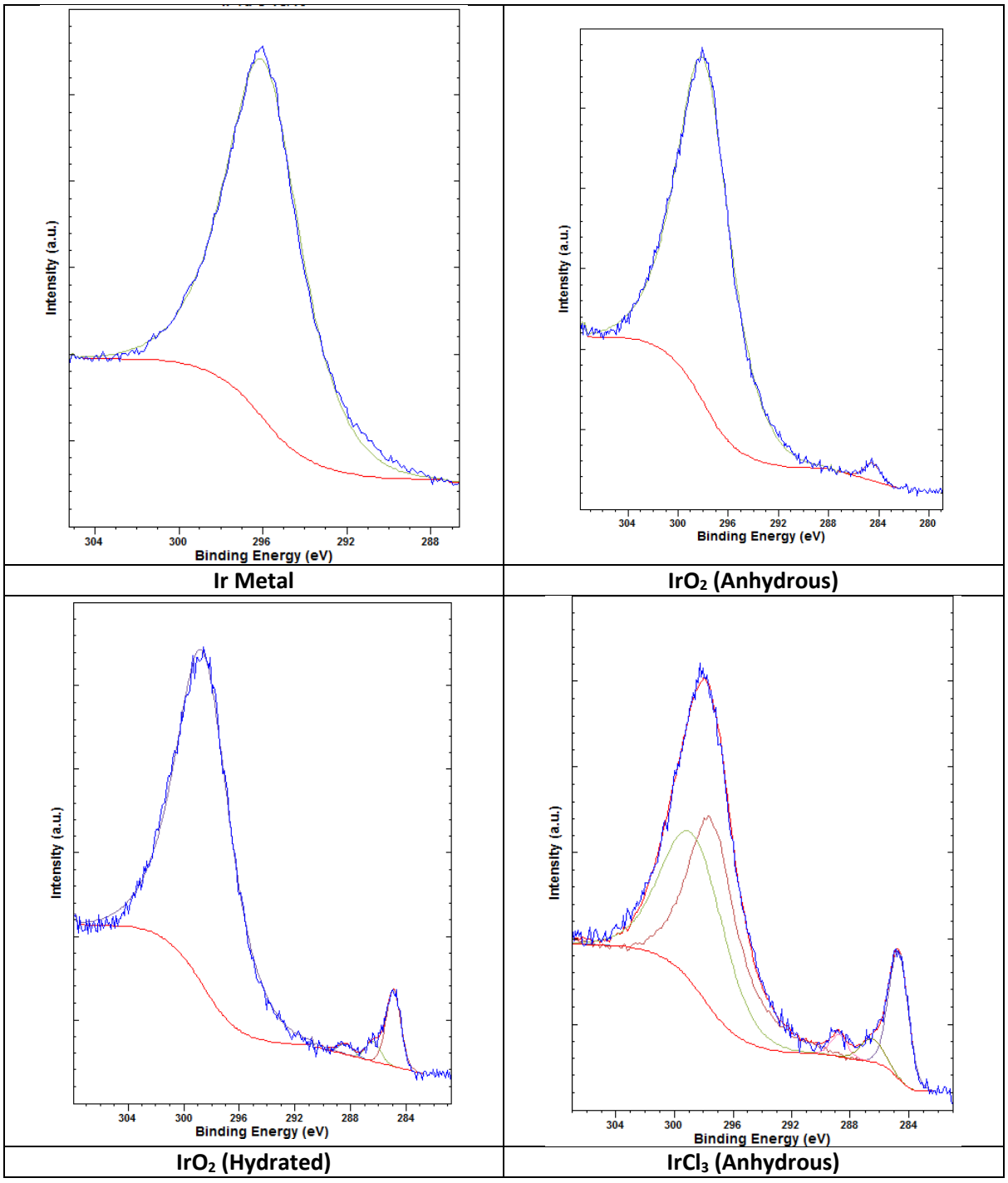

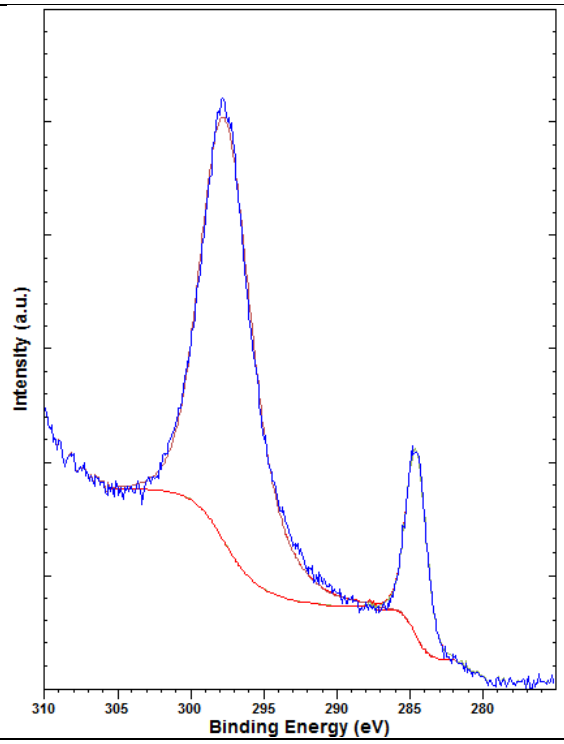

$IrCl_3$ (Hydrated)

Notes:

$IrCl_3$ (Anhydrous) shows fitting using the lineshapes of IrO_2 (hydrated) and $IrCl_3$ Hydrated.

For conducing samples (Ir metal and both oxides), a GL(70) lineshape defines the peak remarkably well.

Fits of carbon region (~285 eV) are also shown where applicable

Fitting of the Ir($4d_{5/2}$) region for each sample analysed in the present study. For all conducting samples (Ir and IrO_2 samples) and simple GL(70) lineshape is sufficient to model the $4d_{5/2}$ peak with satisfactory accuracy for analysis. The broader envelope of the hydrated $IrCl_3$ mirrors that observed for the It(4f) region shown in the main paper in that both IrO_2 and $IrCl_3$ components can be determined.

Figure S4: Survey spectra for each compound indicating the observed peaks and the absence of any unexpected element

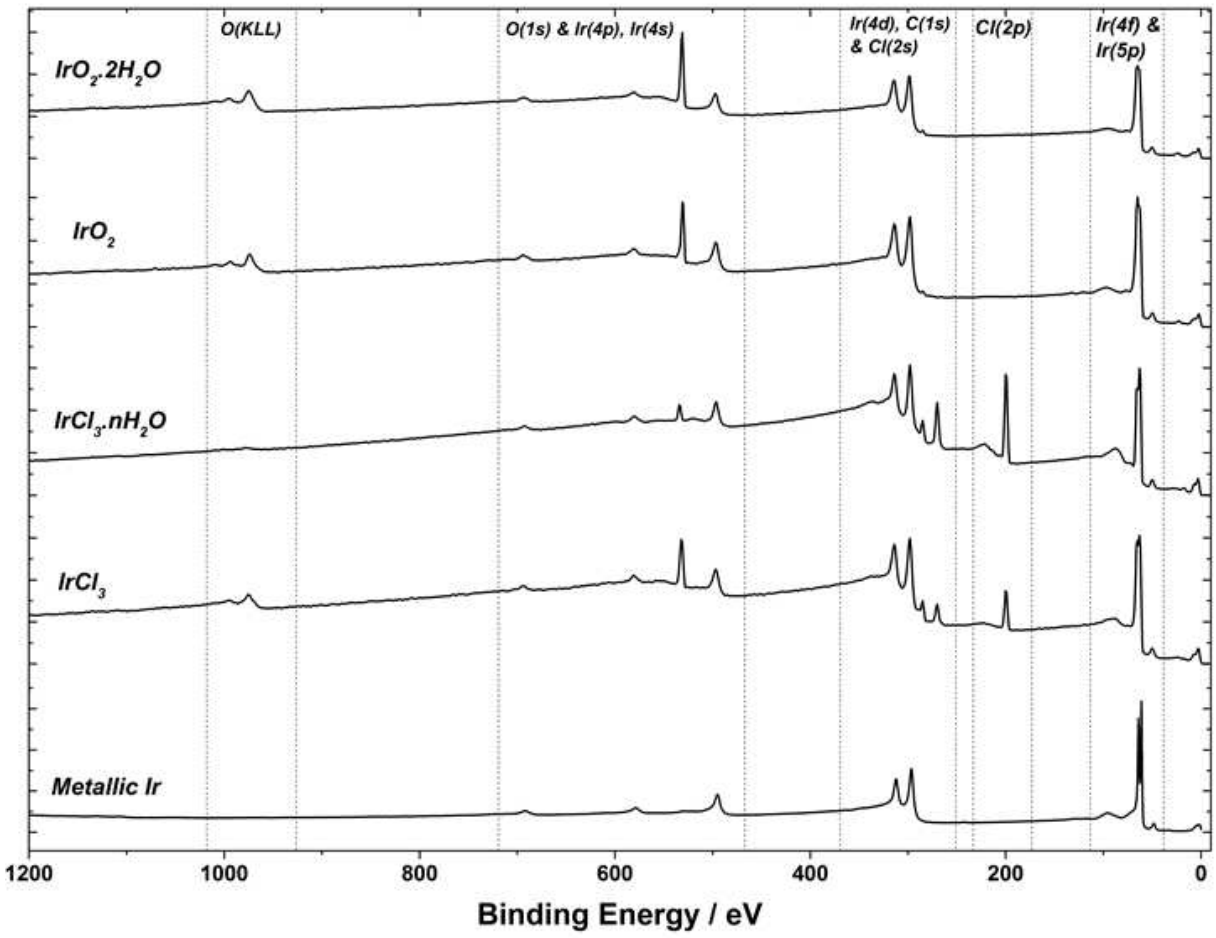

Table S1: Summary of binding energy values observed for the Ir(5p), (4f), (4d) and 4p($_{3/2}$) core-levels in the present study.

Material	Core-level	Binding Energy / eV (±0.2 eV)
Metal	5p3/2	48.1
	5p1/2	63.1
	4f7/2	60.8
	4f5/2	63.8
	4d5/2	296.2
	4d3/2	312.1
	4p3/2	494.8
IrO_2 (Anhydrous)	5p3/2	49.7
	5p1/2	64.7
	4f7/2	61.9
	4f5/2	64.9
	4d5/2	298.1
	4d3/2	313.9
	4p3/2	496.6
IrO_2 (Hydrated)	5p3/2	50.2
	5p1/2	65.2
	4f7/2	62.5
	4f5/2	65.5
	4d5/2	298.6
	4d3/2	314.4
	4p3/2	497.1
$IrCl_3$ (Anhydrous)	5p3/2	49.9
	5p1/2	64.9
	4f7/2	62.4
	4f5/2	65.4
	4d5/2	297.8
	4d3/2	313.6
	4p3/2	496.4
$IrCl_3.nH_2O$	5p3/2	49.7
	5p1/2	64.7
	4f7/2	62.6
	4f5/2	65.6
	4d5/2	298.0
	4d3/2	313.9
	4p3/2	496.3

References

[1] J. Walton, P. Wincott, N. Fairley, A. Carrick, *Peak Fitting with CasaXPS: A Casa PocketBook*, Acolyte Science, Knutsford, UK, **2010**.

[2] V. Pfeifer, T. E. Jones, J. J. Velasco Vélez, C. Massué, R. Arrigo, D. Teschner, F. Girgsdies, M. Scherzer, M. T. Greiner, J. Allan, M. Hashagen, G. Weinberg, S. Piccinin, M. Hävecker, A. Knop-Gericke, R. Schlögl, *Surf Interface Anal* **2016**, *48*, 261.

[3] P. C. Liao, C. S. Chen, W. S. Ho, Y. S. Huang, K. K. Tiong, *Thin Solid Films* **1997**, *301*, 7.